HHS Public Access

Author manuscript

Mol Cancer Res. Author manuscript; available in PMC 2023 January 06.

Published in final edited form as:

Mol Cancer Res. 2022 July 06; 20(7): 1122–1136. doi:10.1158/1541-7786.MCR-21-0681.

PDZ proteins SCRIB and DLG1 regulate myeloma cell surface CD86 expression, growth, and survival

Tyler Moser-Katz[1], **Catherine M. Gavile**[1], **Benjamin G. Barwick**[1], **Kelvin P. Lee**[2], **Lawrence H. Boise**[1]

[1]Department of Hematology and Medical Oncology, Winship Cancer Institute, Emory University, Atlanta, GA

[2]Melvin and Bren Simon Comprehensive Cancer Center, Indiana University School of Medicine, Indianapolis, Indiana

Abstract

Despite advances in the treatment of multiple myeloma (MM) in the past decades, the disease remains incurable, and understanding signals and molecules that can control myeloma growth and survival are important for the development of novel therapeutic strategies. One such molecule, CD86, regulates MM cell survival via its interaction with CD28 and signaling through its cytoplasmic tail. Although the CD86 cytoplasmic tail has been shown to be involved in drug resistance and can induce molecular changes in MM cells, its function has been largely unexplored. Here, we show that CD86 cytoplasmic tail has a role in trafficking CD86 to the cell surface. This is due in part to a PDZ-binding motif at its C-terminus which is important for proper trafficking from the Golgi apparatus. BioID analysis revealed 10 PDZ-domain containing proteins proximal to CD86 cytoplasmic tail in myeloma cells. Among them, we found the planar cell polarity proteins, SCRIB and DLG1, are important for proper CD86 surface expression and the growth and survival of myeloma cells. These findings indicate a mechanism by which myeloma cells confer cellular survival and drug resistance and indicate a possible motif to target for therapeutic gain.

Implications: These findings demonstrate the importance of proper trafficking of CD86 to the cell surface in myeloma cell survival and may provide a new therapeutic target in this disease.

Introduction

Multiple myeloma, a disease of antibody-producing plasma cells, is the second most common hematologic malignancy in the U.S.[1] In 2020, approximately 32,000 patients were diagnosed with myeloma and 13,000 deaths occurred[2]. Although therapeutic agents such as proteasome inhibitors, immunomodulatory drugs, and targeted antibody treatments have increased median survival rates, efficacy of these agents is still limited, and the majority of patients become drug-resistant and relapse[3–5]. While normal plasma cells are highly reliant on interactions with bone marrow stromal cells for survival, myeloma cells may

Corresponding Author: Lawrence H. Boise, 1365C Clifton Road NE, Suite C4078, Atlanta, GA 30322, Tel. No. 404-778-4724, Fax. No. 404-778-5530, lboise@emory.edu.

Conflict of Interest: The authors declare no potential conflicts of interest.

become extramedullary in advanced stages and can survive and proliferate outside of the bone marrow microenvironment[6–9]. Thus the mechanisms that allow MM cells to become independent of the bone marrow microenvironment are central to understanding how the disease progresses to this terminal treatment refractory stage.

Some clues underlying myeloma cell progression can be found within the bone marrow microenvironment where the pro-survival interactions of myeloma cells with stromal cells and the extracellular matrix have been previously studied[6,10–12]. One such stromal-myeloma cell interaction involves the binding of myeloma cell receptor CD28 to CD80/CD86 of a dendritic cell[13]. This CD80/CD86-CD28 interaction is primarily known in context of T-cell co-stimulatory response. During this process, the T cell receptor (TCR) is first activated by MHC peptide complex of an antigen presenting cell (APC), and CD80/86 expressed on APCs binds to T cell CD28 to provide co-stimulation to maximally activate T cell proliferation, and survival[14–18]. Since most myeloma cells co-express CD28 and CD86, we hypothesized a similar role for the proteins in myeloma cells. Specifically, because the CD86-CD28 interaction promotes survival in T cells, this suggests a possible mechanism by which myeloma cells survive independent of stromal cell signals. This pathway could represent a therapeutic target in myeloma, especially as the U.S. Food and Drug Administration has already approved inhibitors of the CD86-CD28 interaction (CTLA4-Ig) for treatment of graft-host rejection and autoimmune disorders[19–22].

CD86 has been primarily characterized as a ligand of CD28, and numerous CD28 signaling motifs and pathways have been identified[23–26]. However, recent work on B cell function in mice[27–33] and dendritic cells[34] demonstrates that CD86 also signals upon ligation to initiate specific responses. Consistent with this, our lab has recently shown that CD86 is necessary for myeloma cell survival and drug resistance[13,35]. The cytoplasmic region of CD86 is important for conferring these effects as well as inducing molecular changes in myeloma cells such as upregulation of IRF4, ITGB1, and ITGB7[35]. This suggests that proper surface expression of CD86 and its downstream signaling is important in myeloma, While a specific polylysine motif in the cytoplasmic tail has been shown to associate CD86 with the cytoskeleton to maintain surface expression in APCs[16], other motifs in the cytoplasmic tail are not known. CD86 contains numerous sites of N-linked glycosylation in its extracellular domain that can direct trafficking to the plasma membrane. However, additional means of regulating CD86 surface expression have remained understudied. Therefore, we set out to further elucidate mechanisms of proper CD86 trafficking in myeloma via its cytoplasmic tail.

Materials and Methods:

Cell Lines

Human Embryonic Kidney 293T (HEK293T) cell line was purchased from American Type Culture Collection (ATCC). Cells were cultured and seeded in 6-well plates containing 2 mL Dulbecco’s modified Eagle’s medium (DMEM; Corning) supplemented with 10% fetal bovine serum (Gemini) at 37 °C in an incubator with 5% CO_2. Myeloma cell lines were cultured as previously described[36]. MM.1s were provided by Dr. Steven Rosen (City of Hope, Duarte, CA), KMS18 were purchased from the Japanese Cell Resource Bank (JCRB),

and RPMI8226 were purchased from ATCC. Cells were cultured in RPMI1640 media supplemented with 10% fetal bovine serum at 37 °C in an incubator with 5% CO_2. Cell lines were *Mycoplasma* tested using PCR-based *Mycoplasma* testing service from ATCC. RPMI8226 and HEK293T cells were most recently tested for *Mycoplasma* in January, 2022 while KMS18 and MM.1s were most recently tested in July, 2021. Cells were passaged for 4–6 weeks and experiments were performed between 1–6 weeks following thaw. Identity of myeloma cells was validated by STR. This was repeated for the KMS18 and RPMI8226 cells after introduction of the Cas9 vector to assure these cells were of the correct origin

Transient Transfection

HEK293T cells were seeded on coverslips on a six-well plate. The next day, they were transfected using Lipofectamine-2000 (Invitrogen) according to manufacturer's instructions after reaching a confluency of 70–90%. Forty-eight hours after transfection, cells were either lysed for protein extraction or fixed for immunofluorescence. Cells were transfected with CD80 (Genscript) and CD86 constructs cloned into pcDNA3.1+ plasmid as previously described[35].

Protein Extraction and Immunoblotting

Cell pellets were lysed in radioimmunoprecipitation assay (RIPA) buffer with protease and phosphatase inhibitors as previously described[9]. Lysates were quantified using the bicinchoninic acid assay (ThermoFisher), and lysates were run in sodium dodecyl sulfate–polyacrylamide gel electrophoresis (SDS-PAGE) gels, then blotted as previously described[9]. Primary antibodies used included: Mouse monoclonal α-CD86 (R&D), mouse monoclonal α-β-actin (Sigma), Streptavidin HRP (Millipore) and rabbit polyclonal α-HA (Abcam). The following secondary antibodies were used: anti-mouse immunoglobulin G–horseradish peroxidase (IgG-HRP) and anti-rabbit IgG-HRP (Santa Cruz Biotechnology)

Immunofluorescence

Cells were grown on glass coverslips (Fisher) coated with 5 μg/cm^2 fibronectin unless otherwise specified (Millipore). Twenty-four hours after transfection, cells were fixed with PHEMO buffer (68 mM PIPES, 25 mM HEPES, 15 mM EGTA-Na_2, 3 mM $MgCl_2$**.**$6H_2O$, 10% DMSO, pH 6.8) supplemented with 3.7% formaldehyde (Fisher), 0.05% glutaraldehyde (Fisher) and 0.2% Triton X-100 (Bio-Rad) for permeabilization when indicated. CD86 was labelled by staining with CD86-APC antibody (Caprico Biosciences). CD80 was labelled by staining with CD80-FITC antibody (BD Biosciences). Mannose-6 phosphate receptor was labelled overnight at 4 degrees Celsius using a rabbit polyclonal antibody α-Mannose-6 phosphate receptor provided as a gift from Dr. Paul Luzio (Cambridge Institute for Medical Research)[37]. Other antibodies used were Rabbit α SYNTENIN (Abcam), Rabbit α SCRIB (Cell signaling) and Rabbit α DLG1 (Thermo Fisher), Mouse α EEA1(BD Biosciences). Goat α rabbit Alexa Fluor 488 (Invitrogen) or Goat α Mouse Alexa Fluor 488 secondary antibody was used to stain cells for 1 hour at room temperature. Coverslips were then mounted on microslides (Fisher) using Prolong Gold containing 300 nM 4′−6-diamidino-2-phenylindole dilactate (DAPI;Invitrogen). Cells were imaged using a Leica TCS SP8 inverted confocal microscope (63X oil HC PL APO, NA 1.4). Mander's

correlation coefficient was analyzed for five cells in three independent assays (15 cells total) and determined using Co-localization tool on FIJI ImageJ.

BioID

For BioID analysis, 50 million cells of MM.1s BirHA or MM.1s CD86-BirHA were cultured in 150 cm^2 flasks. Subsequent BioID was performed as previously described[38]. Gene ontology was performed using String.db. PDZ domain-containing proteins were identified using the HUGO nomenclature online database.

In Situ Proximity Ligation Assay (PLA)

SCRIB/CD86 and DLG1/CD86 interactions were detected in situ using Duolink™ II secondary antibodies and detection kits (Sigma–Aldrich, #DUO92002, #DUO92004, and #DUO92008) according to the manufacturer's instructions. Briefly, PLA probes and primary antibodies: Rabbit α HA (Abcam), Mouse α SYNTENIN (Abnova) Mouse α SCRIB (GeneTex), and Mouse α SAP97/DLG1 (Santa Cruz) were applied to fixed cells. Then, Duolink™ secondary antibodies were added. Polymerase and amplification buffer were added to amplify a positive signal (red dot) and detected by confocal microscopy. DAPI was used for counterstaining of the nucleus.

Real Time Polymerase Chain Reaction (RT-PCR)

RNA was extracted and quantitative reverse transcription polymerase chain reaction (qRT-PCR) was performed as previously described using Applied Biosystems High Capacity cDNA Reverse Transcription Kit (Life Technologies)[36]. Resulting cDNA was amplified using the TaqMan Gene Expression Master Mix (Life Technologies) on the CFX96 Real-Time PCR System following the manufacturer's protocol (Bio-Rad). Probes used were Glyceraldehyde-3-phosphate dehydrogenase, SYNTENIN, CD86, SCRIB, DLG1, and IRF4 (Applied Biosystems).

Flow Cytometry and Analysis

Cell-surface expression CD86-APC (Caprico Biosciences) and integrin β7-PE (BD Biosciences) were measured via flow cytometry. 100,000 live cells were collected, washed with 1× PBS, and stained with appropriate antibodies in 50 μL FACS staining buffer. After incubation of 15 min at 4°C in the dark, cells were washed in 1× PBS and resuspended in 400 μL FACS staining buffer. Samples were run on a FACS Symphony A3 Flow Cytometer (BD Biosciences) and analyzed using FlowJo software.

Generation of Cas9-inducible cell lines and determination of sgRNA

Inducible Cas9 expressing cells were generated using the pCW-Cas9 plasmid through lentiviral infection[39]. Virus was produced by transfecting HEK293T cells with pCW-Cas9 (gift from Eric Lander and David Sabatini: Addgene plasmid # 50661) and packaging plasmids DR8 and VSVg using Lipofectamine 2000[40]. Lentiviral infection and selection of cells were performed as previously described[39]

CD86, SYNTENIN, SCRIB, and DLG1 sgRNA clones were generated by designing specific sgRNAs using the online CRISPOR tool[41] and cloning them into pLX-sgRNA

(gift from Eric Lander and David Sabatini: Addgene plasmid # 50662) using the following primers: GTCGAGTGTGCTACTCAACTCGTTTTAGAGCTAGAAATAGCAA (forward) and GAGTTGAGTAGCACACTCGACGGTGTTTCGTCCTTTCC (reverse). The sgRNA sequences are provided in Supplemental Table 1. Virus generation and infection of inducible Cas9 cells were as described[39]. Twenty-four hours after infection, 10 μg/mL blasticidin was added to select cells for 7 days.

Cell Count Proliferation Assay

KMS18 and RPMI8226 Cas9 inducible cells were infected with sgRNA containing lentiviral particles as described above. The following day, live cells were counted using 100 μL of cells and 100 μL of FITC-conjugated counting beads (Thermo Fisher) and run on a FACS Symphony A3 Flow Cytometer (BD Biosciences). 100,000 live cells were then seeded on 24-well plates in 2 mL of complete media. Doxycycline hyclate (1 μg /mL; Sigma) was then added to cells and counts were repeated using FITC-conjugated counting beads as per the manufacturer's instructions for seven days.

Apoptosis Assays

Cell death was measured by annexin V-fluorescein isothiocyanate (BioVision) and propidium iodide (PI) staining as previously described[36].

Statistical Analysis

Statistical significance was assessed using two-tailed Student *t* test using GraphPad Prism.

Results

CD86 cytoplasmic tail is important for trafficking to cell surface

We previously generated RPMI8226 myeloma cell lines which stably overexpress full length CD86 (CD86FL) or a "tail-less" mutant of CD86 (CD86TL)[35]. CD86TL expresses the extracellular and transmembrane domain and 7 amino acids of the cytosolic domain (Fig 1A). We used vectors coding for CD86FL and CD86TL and transiently transfected them into HEK293T, a cell line which does not endogenously express CD86. We then stained fixed cells with a CD86 antibody to determine CD86 localization 2 days after transfection (Fig 1B). While CD86FL can be observed at the perimeter of the CD86FL cells, CD86TL formed a more diffuse staining pattern with several puncta inside the cells. To verify that this phenotype was not due to a discrepancy in transfection efficiency, we took lysates of these cells and performed western blot analysis. There was no decrease in CD86 total protein expression and in fact, the CD86TL expression was significantly higher than CD86FL (Fig 1C). We also determined that the stable RPMI8226-CD86FL myeloma cells also produced a uniform stain around the perimeter while the RPMI8226-CD86TL myeloma cell lines had more punctate staining (Fig 1D). In order to determine what stage CD86 trafficking to the surface is inhibited, we co-stained the HEK293T cells with Mannose-6 phosphate receptor (M6PR), a Golgi marker, as well as CD86 (Fig 1E). We then analyzed co-localization of these proteins using a Mander's correlation coefficient and observed a significant increase in co-localization between M6PR and CD86 in the CD86TL compared to CD86FL transfected HEK293T (Fig 1F). Since CD86 is glycosylated, we would expect it to be exported from the

Golgi under normal conditions following its synthesis and post-translational modifications. The presence of CD86 in the Golgi apparatus could indicate a defect in anterograde trafficking or increased retrograde trafficking. Therefore, we used a pulse-chase experiment utilizing cell surface biotin labeling to measure rates of CD86 delivery to the plasma membrane following trypsin cleavage. We observed that CD86FL was able to repopulate the cell surface after 1 hour while CD86TL exhibited delayed recovery (Fig S1A). To determine if truncation of the CD86 cytoplasmic tail results in increased retrograde trafficking, we also co-stained with CD86 and an endosomal marker, early endosomal antigen-1 (EEA1) and saw no significant difference in co-localization with CD86 in CD86FL and CD86TL transfected lines (Fig S1B). Together, these data show that the cytoplasmic tail has a role in conferring proper transport of CD86 from the Golgi apparatus to the membrane.

Multiple regions of the CD86 cytoplasmic tail are important for anterograde trafficking

The cytoplasmic region of CD86 is composed of a 61 amino acid long tail. Since we detected a trafficking defect in the CD86TL-transfected HEK293T, we defined which areas of the tail are important for CD86 trafficking. Homology alignment of human CD86 to other higher mammalian species identified numerous conserved and potentially important areas of the cytoplasmic tail[35]. Full length CD86 is 329 amino acids in length, and there may be multiple motifs working in conjunction along the protein to regulate trafficking. Therefore, instead of mutating specific motifs, we developed CD86 truncation mutants that were 282 (CD86Δ282) 298 (CD86Δ298), and 315 (CD86Δ315) amino acids long respectively (Fig 2A). We then transfected the truncation mutants into HEK293T cells and observed CD86 trafficking 2 days following transfection (Fig 2B). While the truncation mutants trafficked CD86 more effectively than CD86TL, none were able to fully phenocopy CD86FL. To determine what point the trafficking is inhibited, we co-stained M6PR and CD86 in pcDNA3.1 vector control, CD86FL, CD86Δ282, CD86Δ298, and CD86Δ315 transfected cells (Fig 2C). When we quantified co-localization using a Mander's correlation coefficient, we observed that the truncation mutants each had significantly higher co-localization of M6PR and CD86 compared to CD86FL (Fig 2D). Furthermore, there is less co-localization the longer the tail, suggesting that there are several regions of the tail that are important for proper CD86 trafficking.

CD86 contains a PDZ binding motif important for surface expression

Since full-length CD86 contains 329 total amino acids, and the CD86Δ315 mutant improperly traffics, we identified 14 amino acids at the C-terminus of CD86 to further dissect. Among higher order mammalian species, CD86 contains a conserved class I Psd95/DLG1/zo-1 (PDZ) binding motif at its C-terminus (Fig 3A). A class I PDZ binding motif is composed of a S/T-X-ϕ motif where X represents any amino acid and ϕ represents a hydrophobic residue[42], and human CD86 C-terminus meets these criteria with TCF at its C-terminus. This motif is commonly found at the C-terminus of receptor proteins and is recognized by adaptor proteins that contain a PDZ domain. PDZ proteins can then perform numerous signaling or scaffolding functions specific to cell and context[42].

To determine whether the PDZ binding motif has a role in cellular trafficking of CD86, we developed a truncation mutant which lacks the final 3 amino acids of CD86, effectively

truncating the PDZ binding motif (CD86Δ326). We then transfected this construct into HEK293T and co-stained with M6PR and CD86 2 days after transfection (Fig 3B). After quantification of co-localization using a Mander's correlation coefficient, we observed significantly more co-localization of M6PR and CD86 in the CD86Δ326 HEK293T compared to CD86FL, illustrating that the PDZ binding motif is important for proper CD86 trafficking to the cell surface (Fig 3C).

Like CD86, CD80 is another receptor protein classically recognized to be involved in the T-cell co-stimulatory response[14]. Unlike CD86, CD80 is not expressed in myeloma cells, so the two proteins may not have redundant roles. Interestingly human CD80 does not contain a PDZ binding motif, thereby suggesting a further difference in trafficking between the two proteins in immune cells (Fig S2A). We developed a "tail-less" mutant of CD80 to assay whether CD80 cytoplasmic tail also confers a proper trafficking phenotype (Fig S2B). When we transfected HEK293T with CD80FL and CD80TL we observed no notable difference in trafficking between the two proteins, illustrating a different mechanism of transport between the two proteins (Fig S2C).

BioID proximity assay identifies numerous CD86 interacting partners

In order to determine possible interacting partners for the CD86 cytoplasmic tail, we utilized the BioID proximity-based labeling assay. This method utilizes a constitutively active biotin ligase (BirA) that is engineered to biotinylate proteins within 10 nm of it[38]. We developed a construct with BirA containing an HA tag (BirHA) cloned into the CD86 tail prior to the PDZ domain (CD86-BirHA) (Fig S3A). We transfected soluble BirHA or CD86-BirHA into the myeloma cell line, MM.1s, resulting in stable cell lines expressing either protein (Fig 4A, Fig S3B). We then used streptavidin-conjugated beads to pull down proximal proteins in either cell line (Fig S3C). On-bead trypsin digestion was performed and unique peptides were analyzed using mass spectrometry.

Proteins were then stratified based on peptide-spectrum match (PSM) score. This assigns a numerical value that expresses the likelihood that fragmentation of a peptide is contained in the experimental spectrum[43]. Proteins with a PSM score of greater than 5 met the determined threshold for a positive hit. Proteins were then deemed to be enriched in the CD86 cytoplasmic tail if a threefold higher PSM score in MM.1s CD86-BirHA was observed in comparison to MM.1s BirHA. In total, there were 225 proteins that were associated with the CD86 cytoplasmic tail (Supplementary Table 2). Using the online database, string.db, we performed gene ontology analyses for KEGG pathway analysis and Reactome Pathways (Fig 4B) and found that the top hits for each pathway were Endocytosis in KEGG (FDR=9.34×10^{-6}) and Membrane Trafficking in Reactome Pathways (FDR=1.13×10^{-5}). The Reactome Pathways analysis also revealed additional functions such as Receptor Tyrosine Kinase signaling, Rho GTPases, glycosylation, intra-Golgi and retrograde Golgi-ER traffic, and COPI-mediated anterograde transport which providing additional information about the biological processes controlled by CD86 binding partners.

We next determined how many of the stratified hits were PDZ domain-containing proteins. Using the HUGO nomenclature online database, we identified 152 known PDZ domain-containing proteins and cross-referenced them with our 225 enriched proteins. Ten

proteins with PDZ domains were found among our hits: SLC9A31, SCRIB, SYNTENIN, PDLIM, PARD3, GORASP2, CASK, AHNAK, DLG1, and ERBB2IP (Fig 4C). Using the CoMMpass dataset, a longitudinal study which follows patient gene expression throughout treatment, we determined that all 10 PDZ domain proteins are expressed to varying degrees in primary myeloma patients (Fig S4A). To stratify proteins to focus, we analyzed patient subtype expression. Both CD86 and CD28 have increased expression in the MAF myeloma subtype[7,35]. We identified SCRIB, AHNAK, and PARD3 as genes with the highest expression in the MAF subtype and DLG1 having the lowest expression in this subtype (Fig S4B). Among the three highest expressing proteins, we decided to focus on SCRIB as it is prognostic of poor patient progression-free and overall survival (Fig S4C). We also wanted to test a PDZ protein that has median relative expression in the MAF subtype and selected SYNTENIN (encoded by SDCBP) as it has been shown to regulate surface levels CD138. CD138 or SYNDECAN is a marker of myeloma cells with a role in myeloma cell adhesion, and we therefore were interested in the potential role of SYNTENIN in myeloma[44]. Furthermore, using the CoMMpass dataset, we observed a positive correlation between SDCBP and CD86 mRNA expression in patients (Fig S4D). Taken together, these proteins may have implications in CD86 expression as well as myeloma cell survival and bone marrow localization, and warranted further exploration.

SCRIB and DLG1 are apical-basal polarity proteins that have been shown to regulate surface levels of numerous proteins[45,46] and have been shown to form complexes with one another to regulate polarity axes of cells[47]. Using a proximity ligation assay (PLA), we verified that SCRIB and DLG1 interact with CD86 while SYNTENIN does not (Fig 4D). We also co-stained CD86-overexpressing RPMI8226 cell lines with CD86 and either SYNTENIN, SCRIB, DLG1, or a secondary antibody-only control (Fig 4E). We compared co-localization of CD86 with either a non-specific secondary antibody-only control, SYNTENIN, SCRIB, or DLG1. While there was no significant difference between SYNTENIN co-localization and the secondary-only control, there was a significant increase in SCRIB and DLG1 co-localization compared with SYNTENIN (Fig 4F). Identification of SCRIB and DLG1 co-localization with CD86 led us to further explore their function in multiple myeloma.

SCRIB and DLG1 regulate CD86 surface expression

We next wanted to elucidate the role of SCRIB and DLG1 in CD86 trafficking to the cell surface. While they have been involved in numerous cancers, their roles in multiple myeloma have been unexplored[48,49]. We utilized myeloma cell lines, KMS18 and RPMI8226, which were engineered to stably express a doxycycline-inducible Cas9 enzyme. Single guide RNA targeting either CD86 (sgCD86), SCRIB (sgSCRIB), and DLG1 (sgDLG1) were generated based on specificity and efficiency using the online CRISPOR tool[41]. As a control, a single guide vector targeting the viral incorporation site, AAVS1, was used (plx-sgRNA)[40]. We used lentiviral particles to infect myeloma cells with sgRNA and then selected for cells containing the plasmids for seven days using blasticidin. Following selection, cells were plated and doxycycline was added to activate the Cas9 enzyme expression (Fig 5A). We have previously determined a role for CD86 in myeloma cell survival and hypothesized that SCRIB and DLG1 may be involved as well. We therefore did

not establish stable cell lines and instead performed a transient assay measuring cell counts, cell death, and CD86 surface expression for seven days.

We first verified that CD86 surface expression was decreased with the addition of CD86 guides. Indeed, we observed reduced CD86 expression in two guides targeting CD86 as soon as three days after doxycycline addition (Fig 5B). At day three, we also observed decreased CD86 surface expression with three SCRIB guides in KMS18 (Fig 5C–D, 5G, S5A). Similarly, we observed decreased CD86 surface expression in the sgDLG1 KMS18 cells after three days (Fig 5E–G, S5A). While surface levels were decreased, we did not observe any difference in total CD86 protein levels (Fig S5B). We repeated this experiment using two guides against SYNTENIN (sgSYNTENIN) with the hypothesis that CD86 surface expression would not be affected as SYNTENIN does not co-localize with CD86. Indeed, we observed no change in CD86 surface expression (Fig S6A-B). These data suggest that SCRIB and DLG1 affect CD86 surface expression in myeloma, and we wanted to further explore what effect SCRIB KO and DLG1 KO would have on myeloma cells.

SCRIB, DLG1, and SYNTENIN are important for myeloma cell growth and viability

To determine whether knockout of CD86, SYNTENIN, SCRIB, or DLG1 resulted in less proliferation of myeloma cells, we used FITC-conjugated beads and flow cytometry to count live cells 0 to 7 days following doxycycline addition. We conducted these experiments in KMS18 and RPMI8226 myeloma cell lines and found that knockout of CD86, SCRIB, and DLG1 (Fig 6A–C) resulted in significantly diminished cell growth compared to plx-sgRNA control cells. We hypothesized that this decrease in cell count could be largely due to an increase in cell death. We have previously shown using shRNA knockdown that loss of CD86 results in significantly higher cell death in both KMS18 and RPMI8226[35]. Indeed, we saw that knockout of CD86 via CRISPR-Cas9 resulted in increased cell death in both lines (Fig 6D). SCRIB and DLG1 gene editing resulted in an increase in cell death in both cell lines (Fig 6E–F). We also observed decreased cell proliferation and increased cell death in SYNTENIN knockout lines despite the lack of change in CD86 surface expression (Fig S6C-D). This suggests a role for SYNTENIN in myeloma viability that is independent of control of CD86 trafficking.

Interestingly, the majority of cell death occurred during days 1–3 in all knockout lines. This is particularly evident in RPMI8226 lines where approximately 80% of all knockout cells die by day 3 (Fig 6D–F, Fig S7A-B). RPMI8226 are largely dependent on CD86 for survival[35], and the majority of CD86 KO cells die by day 3 (Fig 6D). In the RPMI8226 SCRIB KO and DLG1 KO, a “CD86 low” population fails to grow out, and the few cells that do survive past day 3 have normal protein expression of CD86 (Fig S7B). Furthermore, in the KMS18 SCRIB KO and DLG1 KO, the “CD86 low” populations do not grow out past day 3, and CD86 resurfaces in days 4–7 (Fig S5C). This points to a population of cells that did not efficiently edit CD86 as the population that was able to effectively grow out.

SCRIB and DLG1 facilitate CD86 pro-survival signaling

To further investigate the role that SCRIB and DLG1 had in CD86-mediated cell survival, we co-stained RPMI8226-CD86FL cells with CD86 and either SCRIB or DLG1 (Fig 7A).

Since CD86 signals via cell-cell contact, we hypothesized that there would be a difference in co-localization of CD86 and SCRIB or DLG1 at points of cell contact compared to non-contact sites. Surprisingly, we observed a decrease in SCRIB/DLG1 co-localization with CD86 at sites of contact compared to non-contact sites (Fig 7B). We also noticed that these contact sites had higher expression of CD86 in the RPMI8226-CD86FL cell lines (Fig 4E, 7C). We hypothesized that binding of CD86 to CD28 on myeloma cells stabilizes CD86 expression and allows SCRIB and DLG1 to leave. Consistent with this possibility, CD86FL-transfected HEK293T, a cell line which does not express CD28, displayed no difference in CD86 expression in contact sites compared to non-contact sites (Fig 7C–D). To verify whether the cell death in the SCRIB and DLG1 knockout lines was due in part to the lack of a CD86-intrinsic signal we determined if loss of the PDZ domain proteins shared other characteristics with the loss of CD86. We have previously shown that loss of CD86 in myeloma cell lines leads to decreased expression of IRF4 and Integrin β7[35], two proteins which have been implicated in myeloma cell survival[50,51]. We quantified mRNA expression of IRF4 in our CD86, SCRIB, and DLG1 RPMI8226 knockout lines and observed a significant decrease with every sgCD86 and sgSCRIB line and 2 out of 3 DLG1 sgRNAs (Fig 7E). Additionally, integrin β7, decreased in all CD86, SCRIB, and DLG1 sgRNAs 2 days following doxycycline addition (Fig 7F). This suggests that the decrease in CD86 surface expression observed with the loss of SCRIB or DLG1 results in a decrease in CD86-mediated growth and survival signaling. To verify that loss of CD86 signaling is important for SCRIB KO and DLG1 KO-induced cell death, we overexpressed CD86FL in SCRIB KO and DLG1 KO RPMI8226 cells and observed that dominant CD86 expression rescues cell death induced by SCRIB/DLG1 ablation (Fig 7G, S7C).

Discussion

Interaction between CD28 and CD86 on myeloma cells facilitates myeloma cell survival in a bone marrow independent niche. We previously demonstrated a role for the CD86 cytoplasmic tail in drug resistance and induction of molecular changes in myeloma cells. This study illustrates how the CD86 cytoplasmic tail mediates effective trafficking of the protein to the cell surface. We took advantage of a cell line lacking endogenous CD86 to monitor trafficking of full-length CD86 or a tail-less mutant of CD86 and observed a clear difference in efficiency of CD86 to traffic to the plasma membrane. We have shown that lacking the tail results in accumulation of CD86 at the Golgi apparatus, and KEGG pathway analysis has revealed numerous proteins involved in endocytosis in proximity to CD86 cytoplasmic tail. While retrograde trafficking may play a role in CD86 surface expression, the lack of difference in EEA1 co-localization between CD86FL and CD86TL transfected HEK293T suggest that the tail primarily affects anterograde trafficking.

The CD86 cytoplasmic tail is 61 amino acids long and makes up almost 20% of the protein sequence. It follows that there may be numerous regions that can be possible binding regions for intracellular proteins to influence trafficking. Since the length of the tail inversely corresponds with the amount of CD86 that co-localizes with M6PR, we hypothesize that a variety of proteins may be binding to the tail at different locations to influence CD86 localization both inside and outside of the Golgi. Additionally, KMS18 cytoplasmic tail contains a SNP resulting in a A304T change whereas MM.1s and RPMI8226 have an allele

that is conserved among higher order mammalian species. This polymorphism is associated with increased cancer risk and allograft rejection, illustrating the importance for further study of various regions of the CD86 cytoplasmic tail[52–54].

The discovery of a PDZ-binding motif at the C-terminus provides clues as to how the protein is being regulated. PDZ domain proteins have been largely studied and have numerous context-dependent roles in a variety of cell types. The difference in trafficking effectiveness between full-length CD86 and CD86 lacking the PDZ binding motif in HEK293T shows the importance of this motif for proper surface transport. The existence of the PDZ binding motif on CD86 but not CD80 and lack of importance of CD80 tail in trafficking to the surface may also provide clues in antigen presenting cells toward the preferential expression of either CD80 or CD86 during T-cell co-stimulation. While the CD80 cytoplasmic tail does not seem to be necessary for trafficking to the surface, it has previously been shown to influence CD80 localization at the cell surface during T cell co-stimulation[15,55]. Interestingly, ICAM-1, another receptor protein that is involved in both myeloma cell adhesion[56] and immunological signaling[57] contains a PDZ binding motif. SYNDECAN-1 (CD138) is yet another PDZ binding motif-containing protein whose surface levels have previously been shown to be regulated by SYNTENIN[44]. CD138 is a heparan sulfate proteoglycan important for myeloma cell adhesion, and this may be a means by which SYNTENIN affects myeloma cell growth and survival[58]. The presence of a three-amino acid motif on proteins that are implicated in myeloma growth and survival represents a specific target for potential therapeutic treatment.

We mapped the interaction network of CD86 cytoplasmic tail using the BioID method followed by liquid chromatography-mass spectrometry. Among our enriched proteins, ten of them contained PDZ domains. Of these ten PDZ domain proteins, half of them (CASK, DLG1, PARD3, PDLIM, SCRIB) are involved in cell polarity. All of these five proteins except PDLIM have been shown to interact with one another[59–61]. A recent study found that SCRIB can regulate CD86 surface levels in activated antigen presenting cells[62]. Our findings expand this research to malignant plasma cells, identify a role for DLG1 in CD86 regulation as well, and determine a novel outcome of this process in regulating myeloma growth and survival.

One notable enriched protein in the interactome without a PDZ domain was SLC3A2. This protein makes up the heavy chain of CD98, which is a determinant of IMiD activity in multiple myeloma[63]. IMiDs are cytostatic drugs that halt proliferation in myeloma. We have also previously found that CD98 light chain (SLC7A5) is significantly downregulated in both CD28 and CD86-silenced cells. Since our data suggest that CD86 may have a role in proliferation, the functional interaction between CD86 and CD98 in myeloma warrants further investigation.

The similar phenotype of decreased CD86 surface expression in SCRIB KO and DLG1 KO cells suggests that these proteins may be forming a complex with one another. Alternatively, they could be part of a larger complex which regulates CD86 membrane trafficking and localization. The classical function of these two proteins may underlie that not only the amount of CD86 surface expression but also its location is important for maintenance of

cellular survival. For example, CD86 surface expression at points of cell-cell contact appears to be higher (Fig 4E, 7C–D). Furthermore, we found a decrease in co-localization between CD86 and SCRIB/DLG1 in areas of cell contact (Fig 7A–B). This suggests that SCRIB and DLG1 may be helping to traffic CD86 to areas of the cell surface where it can bind to CD28. Binding to CD28 then stabilizes CD86 surface expression and can allow SCRIB and DLG1 to leave the site of contact to perform other roles in the cell.

Our data also show that SCRIB and DLG1 are important for cell growth and viability in multiple myeloma cell lines, KMS18 and RPMI8226. The majority of cell death appears to take place within the first four days of doxycycline addition in both cell lines. Interestingly, in KMS18 we start to see expression of CD86 decrease by day 2 in our CD86 KO, SCRIB KO, and DLG1 KO. However, following day 4, the “CD86-low” population in the SCRIB KO and DLG1 KO do not grow out while a population of cells with normal expression of CD86 survives and proliferates. We see this to a greater effect in RPMI8226, a cell line that is more dependent on CD86. In this line, a CD86-low population is unable to grow out and roughly 80% of SCRIB/DLG1 KO cells die by day 3. The decrease of IRF4 and Integrin β7 expression in the SCRIB/DLG1 KO cells and rescue of cell mortality via dominant CD86-expression point to the lack of CD86 signaling as a mechanism by which these cells die. Since we have also shown a role for CD28 in both normal and malignant plasma cell survival, we cannot rule out a role for diminished CD28 signaling as a result of lower CD86 surface expression contributing to cell death as well[26]. The presence of a population of normally expressing CD86 cells is likely due to incomplete gene editing, however it remains possible that activation of a compensatory mechanism to maintain CD86 surface expression in a small fraction of cells may occur. Additionally, SCRIB and DLG1 have pleiotropic roles and may also be conferring myeloma cell survival via additional mechanisms.

Taken together, our data identify a means of CD86 transport and expression at the surface of myeloma cells. It illustrates that SCRIB and DLG1 are two polarity proteins expressed in myeloma that can transport CD86 to the membrane. Proper transport is reliant on a complete cytoplasmic tail with a PDZ binding motif at its C-terminus. Ablation of SCRIB or DLG1 results in a decrease in CD86 surface expression, myeloma cell survival, and proliferation. These results elucidate a role for PDZ proteins in regulation of myeloma growth and may provide new insights for targeted therapeutic advances in multiple myeloma.

Supplementary Material

Refer to Web version on PubMed Central for supplementary material.

Acknowledgments:

This work was supported by R01 CA121044 (K.P.L.), R01 CA192844 (L.H.B.), and Paula and Rodger Riney Foundation (L.H.B.). B.G.B. was supported by Developmental Funds from Winship Cancer Institute of Emory University, post-doctoral fellowship PF-17-109-1-TBG from the American Cancer Society, a Research Fellow Award from the MMRF, and American Society of Hematology Scholar Award. Research reported in this publication was supported in part by the Pediatrics/Winship Flow Cytometry Core of Winship Cancer Institute of Emory University, Children’s Healthcare of Atlanta and NIH/NCI under award number P30CA138292.

Research reported in this publication was also supported in part by the Emory Integrated Genomics Core (EIGC), Emory Integrated Proteomics Core, and Integrated Cellular Imaging shared resources of Winship Cancer Institute of

Emory University and NIH/NCI under award number P30CA138292. The content is solely the responsibility of the authors and does not necessarily represent the official views of the National Institutes of Health.

We thank Dr. Vikas Gupta for generation of the KMS18 and RPMI8226 Cas9 cell lines. We also thank Drs. Rachel Turn and Richard Kahn for antibodies used for immunofluorescence and their assistance and Dr. Andrew Kowalczyk for assistance with the biotin pulse chase surface labeling experiment.

References

(1). Rajkumar SV Multiple Myeloma: 2016 Update on Diagnosis, Risk-Stratification, and Management. Am. J. Hematol 2016, 91 (7), 719–734. 10.1002/ajh.24402. [PubMed: 27291302]

(2). Myeloma - SEER Stat Fact Sheets http://seer.cancer.gov/statfacts/html/mulmy.html.

(3). Kumar SK; Rajkumar SV; Dispenzieri A; Lacy MQ; Hayman SR; Buadi FK, et al. Improved Survival in Multiple Myeloma and the Impact of Novel Therapies. Blood 2008, 111 (5), 2516–2520. 10.1182/blood-2007-10-116129. [PubMed: 17975015]

(4). Attal M; Harousseau JL; Stoppa AM; Sotto JJ; Fuzibet JG; Rossi JF et al. Prospective, Randomized Trial of Autologous Bone Marrow Transplantation and Chemotherapy in Multiple Myeloma. Intergroupe Français Du Myélome. N. Engl. J. Med 1996, 335 (2), 91–97. 10.1056/NEJM199607113350204. [PubMed: 8649495]

(5). Boise LH; Kaufman JL; Bahlis NJ; Lonial S; Lee KP The Tao of Myeloma. Blood 2014, 124 (12), 1873–1879. 10.1182/blood-2014-05-578732. [PubMed: 25097176]

(6). Bahlis NJ; King AM; Kolonias D; Carlson LM; Liu HY; Hussein MA et al. CD28-Mediated Regulation of Multiple Myeloma Cell Proliferation and Survival. Blood 2007, 109 (11), 5002–5010. 10.1182/blood-2006-03-012542. [PubMed: 17311991]

(7). Nair JR; Carlson LM; Koorella C; Rozanski CH; Byrne GE; Bergsagel PL et al. CD28 Expressed on Malignant Plasma Cells Induces a Prosurvival and Immunosuppressive Microenvironment. J. Immunol 2011, 187 (3), 1243–1253. 10.4049/jimmunol.1100016. [PubMed: 21715687]

(8). Rozanski CH; Arens R; Carlson LM; Nair J; Boise LH; Chanan-Khan AA; Schoenberger SP; Lee KP Sustained Antibody Responses Depend on CD28 Function in Bone Marrow–Resident Plasma Cells. Journal of Experimental Medicine 2011, 208 (7), 1435–1446. 10.1084/jem.20110040. [PubMed: 21690252]

(9). Gupta VA; Matulis SM; Conage-Pough JE; Nooka AK; Kaufman JL; Lonial S et al. Bone Marrow Microenvironment Derived Signals Induce Mcl-1 Dependence in Multiple Myeloma. Blood 2017. 10.1182/blood-2016-10-745059.

(10). Damiano JS; Cress AE; Hazlehurst LA; Shtil AA; Dalton WS Cell Adhesion Mediated Drug Resistance (CAM-DR): Role of Integrins and Resistance to Apoptosis in Human Myeloma Cell Lines. Blood 1999, 93 (5), 1658–1667. [PubMed: 10029595]

(11). Zheng Y; Cai Z; Wang S; Zhang X; Qian J; Hong S et al. Macrophages Are an Abundant Component of Myeloma Microenvironment and Protect Myeloma Cells from Chemotherapy Drug-Induced Apoptosis. Blood 2009, 114 (17), 3625–3628. 10.1182/blood-2009-05-220285. [PubMed: 19710503]

(12). Moser-Katz T; Joseph NS; Dhodapkar MV; Lee KP; Boise LH Game of Bones: How Myeloma Manipulates Its Microenvironment. Front. Oncol 2021, 10. 10.3389/fonc.2020.625199.

(13). Murray ME; Gavile CM; Nair JR; Koorella C; Carlson LM; Buac D et al. CD28-Mediated pro-Survival Signaling Induces Chemotherapeutic Resistance in Multiple Myeloma. Blood 2014, 123 (24), 3770–3779. 10.1182/blood-2013-10-530964. [PubMed: 24782505]

(14). Linsley PS; Brady W; Grosmaire L; Aruffo A; Damle NK; Ledbetter JA Binding of the B Cell Activation Antigen B7 to CD28 Costimulates T Cell Proliferation and Interleukin 2 MRNA Accumulation. J. Exp. Med 1991, 173 (3), 721–730. [PubMed: 1847722]

(15). Tseng S-Y; Liu M; Dustin ML CD80 Cytoplasmic Domain Controls Localization of CD28, CTLA-4, and Protein Kinase Ctheta in the Immunological Synapse. J. Immunol 2005, 175 (12), 7829–7836. [PubMed: 16339518]

(16). Girard T; El-Far M; Gaucher D; Acuto O; Beaulé G et al. A Conserved Polylysine Motif in CD86 Cytoplasmic Tail Is Necessary for Cytoskeletal Association and Effective Co-Stimulation.

Biochem. Biophys. Res. Commun 2012, 423 (2), 301–307. 10.1016/j.bbrc.2012.05.116. [PubMed: 22659416]

(17). Comrie WA; Burkhardt JK Action and Traction: Cytoskeletal Control of Receptor Triggering at the Immunological Synapse. Front Immunol 2016, 7, 68. 10.3389/fimmu.2016.00068. [PubMed: 27014258]

(18). Mukherjee S; Maiti PK; Nandi D Role of CD80, CD86, and CTLA4 on Mouse CD4+ T Lymphocytes in Enhancing Cell-Cycle Progression and Survival after Activation with PMA and Ionomycin. Journal of Leukocyte Biology 2002, 72 (5), 921–931. 10.1189/jlb.72.5.921. [PubMed: 12429713]

(19). Vincenti F; Rostaing L; Grinyo J; Rice K; Steinberg S; Gaite L et al. Belatacept and Long-Term Outcomes in Kidney Transplantation. N. Engl. J. Med 2016, 374 (4), 333–343. 10.1056/NEJMoa1506027. [PubMed: 26816011]

(20). Kirk AD; Harlan DM; Armstrong NN; Davis TA; Dong Y; Gray GS et al. CTLA4-Ig and Anti-CD40 Ligand Prevent Renal Allograft Rejection in Primates. Proc. Natl. Acad. Sci. U.S.A 1997, 94 (16), 8789–8794. 10.1073/pnas.94.16.8789. [PubMed: 9238056]

(21). Kremer JM; Westhovens R; Leon M; Di Giorgio E; Alten R; Steinfeld S et al. Treatment of Rheumatoid Arthritis by Selective Inhibition of T-Cell Activation with Fusion Protein CTLA4Ig. N. Engl. J. Med 2003, 349 (20), 1907–1915. 10.1056/NEJMoa035075. [PubMed: 14614165]

(22). Finck BK; Linsley PS; Wofsy D Treatment of Murine Lupus with CTLA4Ig. Science 1994, 265 (5176), 1225–1227. 10.1126/science.7520604. [PubMed: 7520604]

(23). Boomer JS; Green JM An Enigmatic Tail of CD28 Signaling. Cold Spring Harb Perspect Biol 2010, 2 (8), a002436. 10.1101/cshperspect.a002436. [PubMed: 20534709]

(24). Dodson LF; Boomer JS; Deppong CM; Shah DD; Sim J; Bricker TL et al. Targeted Knock-In Mice Expressing Mutations of CD28 Reveal an Essential Pathway for Costimulation. Molecular and Cellular Biology 2009, 29 (13), 3710–3721. 10.1128/MCB.01869-08. [PubMed: 19398586]

(25). Friend LD; Shah DD; Deppong C; Lin J; Bricker TL; Juehne TI et al. A Dose-Dependent Requirement for the Proline Motif of CD28 in Cellular and Humoral Immunity Revealed by a Targeted Knockin Mutant. J Exp Med 2006, 203 (9), 2121–2133. 10.1084/jem.20052230. [PubMed: 16908623]

(26). Rozanski CH; Utley A; Carlson LM; Farren MR; Murray M; Russell LM et al. CD28 Promotes Plasma Cell Survival, Sustained Antibody Responses, and BLIMP-1 Upregulation through Its Distal PYAP Proline Motif. J. Immunol 2015, 194 (10), 4717–4728. 10.4049/jimmunol.1402260. [PubMed: 25833397]

(27). Kasprowicz DJ; Kohm AP; Berton MT; Chruscinski AJ; Sharpe A; Sanders VM Stimulation of the B Cell Receptor, CD86 (B7–2), and the Beta 2-Adrenergic Receptor Intrinsically Modulates the Level of IgG1 and IgE Produced per B Cell. J. Immunol 2000, 165 (2), 680–690. 10.4049/jimmunol.165.2.680. [PubMed: 10878340]

(28). Podojil JR; Sanders VM CD86 and Beta2-Adrenergic Receptor Stimulation Regulate B-Cell Activity Cooperatively. Trends Immunol. 2005, 26 (4), 180–185. 10.1016/j.it.2005.02.005. [PubMed: 15797507]

(29). Podojil JR; Sanders VM Selective Regulation of Mature IgG1 Transcription by CD86 and Beta 2-Adrenergic Receptor Stimulation. J. Immunol 2003, 170 (10), 5143–5151. 10.4049/jimmunol.170.10.5143. [PubMed: 12734361]

(30). Podojil JR; Kin NW; Sanders VM CD86 and Beta2-Adrenergic Receptor Signaling Pathways, Respectively, Increase Oct-2 and OCA-B Expression and Binding to the 3'-IgH Enhancer in B Cells. J. Biol. Chem 2004, 279 (22), 23394–23404. 10.1074/jbc.M313096200. [PubMed: 15024018]

(31). Kin NW; Sanders VM CD86 Regulates IgG1 Production via a CD19-Dependent Mechanism. J. Immunol 2007, 179 (3), 1516–1523. 10.4049/jimmunol.179.3.1516. [PubMed: 17641017]

(32). Rau FC; Dieter J; Luo Z; Priest SO; Baumgarth N B7–1/2 (CD80/CD86) Direct Signaling to B Cells Enhances IgG Secretion. J. Immunol 2009, 183 (12), 7661–7671. 10.4049/jimmunol.0803783. [PubMed: 19933871]

(33). Salek-Ardakani S; Choi YS; Rafii-El-Idrissi Benhnia M; Flynn R; Arens R; Shoenberger S et al. B Cell-Specific Expression of B7–2 Is Required for Follicular Th Cell Function in Response

to Vaccinia Virus. J. Immunol 2011, 186 (9), 5294–5303. 10.4049/jimmunol.1100406. [PubMed: 21441451]

(34). Koorella C; Nair JR; Murray ME; Carlson LM; Watkins SK; Lee KP Novel Regulation of CD80/CD86-Induced Phosphatidylinositol 3-Kinase Signaling by NOTCH1 Protein in Interleukin-6 and Indoleamine 2,3-Dioxygenase Production by Dendritic Cells. J. Biol. Chem 2014, 289 (11), 7747–7762. 10.1074/jbc.M113.519686. [PubMed: 24415757]

(35). Gavile CM; Barwick BG; Newman S; Neri P; Nooka AK; Lonial S et al. CD86 Regulates Myeloma Cell Survival. Blood Adv 2017, 1 (25), 2307–2319. 10.1182/bloodadvances.2017011601. [PubMed: 29296880]

(36). Morales AA; Kurtoglu M; Matulis SM; Liu J; Siefker D; Gutman D et al. Distribution of Bim Determines Mcl-1 Dependence or Codependence with Bcl-XL/Bcl-2 in Mcl-1-Expressing Myeloma Cells. Blood 2011, 118 (5), 1329–1339. 10.1182/blood-2011-01-327197. [PubMed: 21659544]

(37). Reaves BJ; Bright NA; Mullock BM; Luzio JP The Effect of Wortmannin on the Localisation of Lysosomal Type I Integral Membrane Glycoproteins Suggests a Role for Phosphoinositide 3-Kinase Activity in Regulating Membrane Traffic Late in the Endocytic Pathway. J Cell Sci 1996, 109 (Pt 4), 749–762. [PubMed: 8718666]

(38). Roux KJ; Kim DI; Burke B BioID: A Screen for Protein-Protein Interactions. Curr Protoc Protein Sci 2013, 74, 19.23.1–19.23.14. 10.1002/0471140864.ps1923s74. [PubMed: 24510646]

(39). Gupta VA; Barwick BG; Matulis SM; Shirasaki R; Jaye DL; Keats JJ; et al. Venetoclax Sensitivity in Multiple Myeloma Is Associated with B-Cell Gene Expression. Blood 2021, 137 (26), 3604–3615. 10.1182/blood.2020007899. [PubMed: 33649772]

(40). Wang T; Wei JJ; Sabatini DM; Lander ES Genetic Screens in Human Cells Using the CRISPR-Cas9 System. Science 2014, 343 (6166), 80–84. 10.1126/science.1246981. [PubMed: 24336569]

(41). Concordet J-P; Haeussler M CRISPOR: Intuitive Guide Selection for CRISPR/Cas9 Genome Editing Experiments and Screens. Nucleic Acids Research 2018, 46 (W1), W242–W245. 10.1093/nar/gky354. [PubMed: 29762716]

(42). Lee H-J; Zheng JJ PDZ Domains and Their Binding Partners: Structure, Specificity, and Modification. Cell Communication and Signaling 2010, 8, 8. 10.1186/1478-811X-8-8. [PubMed: 20509869]

(43). Frank AM A Ranking-Based Scoring Function For Peptide-Spectrum Matches. J Proteome Res 2009, 8 (5), 2241–2252. 10.1021/pr800678b. [PubMed: 19231891]

(44). Grootjans JJ; Zimmermann P; Reekmans G; Smets A; Degeest G; Dürr J et al. Syntenin, a PDZ Protein That Binds Syndecan Cytoplasmic Domains. Proc Natl Acad Sci U S A 1997, 94 (25), 13683–13688. [PubMed: 9391086]

(45). Sharifkhodaei Z; Gilbert MM; Auld VJ Scribble and Discs Large Mediate Tricellular Junction Formation. Development 2019, 146 (18). 10.1242/dev.174763.

(46). Fahey-Lozano N; La Marca JE; Portela M; Richardson HE Drosophila Models of Cell Polarity and Cell Competition in Tumourigenesis. Adv Exp Med Biol 2019, 1167, 37–64. 10.1007/978-3-030-23629-8. [PubMed: 31520348]

(47). Osmani N; Vitale N; Borg J-P; Etienne-Manneville S Scrib Controls Cdc42 Localization and Activity to Promote Cell Polarization during Astrocyte Migration. Curr Biol 2006, 16 (24), 2395–2405. 10.1016/j.cub.2006.10.026. [PubMed: 17081755]

(48). Cordenonsi M; Zanconato F; Azzolin L; Forcato M; Rosato A; Frasson C et al. The Hippo Transducer TAZ Confers Cancer Stem Cell-Related Traits on Breast Cancer Cells. Cell 2011, 147 (4), 759–772. 10.1016/j.cell.2011.09.048. [PubMed: 22078877]

(49). Zhu G-D; OuYang S; Liu F; Zhu Z-G; Jiang F-N; Zhang B Elevated Expression of DLG1 Is Associated with Poor Prognosis in Patients with Colorectal Cancer. Ann Clin Lab Sci 2017, 47 (6), 657–662. [PubMed: 29263038]

(50). Shaffer AL; Emre NCT; Lamy L; Ngo VN; Wright G; Xiao W et al. IRF4 Addiction in Multiple Myeloma. Nature 2008, 454 (7201), 226–231. 10.1038/nature07064. [PubMed: 18568025]

(51). Neri P; Ren L; Azab AK; Brentnall M; Gratton K; Klimowicz AC et al. Integrin B7-Mediated Regulation of Multiple Myeloma Cell Adhesion, Migration, and Invasion. Blood 2011, 117 (23), 6202–6213. 10.1182/blood-2010-06-292243. [PubMed: 21474670]

(52). Pan X-M; Gao L-B; Liang W-B; Liu Y; Zhu Y; Tang M et al. CD86 +1057 G/A Polymorphism and the Risk of Colorectal Cancer. DNA Cell Biol 2010, 29 (7), 381–386. 10.1089/dna.2009.1003. [PubMed: 20380573]

(53). Xiang H; Zhao W; Sun Y; Qian W; Xing J; Zhou Y et al. CD86 Gene Variants and Susceptibility to Pancreatic Cancer. J Cancer Res Clin Oncol 2012, 138 (12), 2061–2067. 10.1007/s00432-012-1289-9. [PubMed: 22821131]

(54). Marín LA; Moya-Quiles MR; Miras M; Muro M; Minguela A; Bermejo J; et al. Evaluation of CD86 Gene Polymorphism at +1057 Position in Liver Transplant Recipients. Transpl Immunol 2005, 15 (1), 69–74. 10.1016/j.trim.2005.04.003. [PubMed: 16223675]

(55). Doty RT; Clark EA Subcellular Localization of CD80 Receptors Is Dependent on an Intact Cytoplasmic Tail and Is Required for CD28-Dependent T Cell Costimulation. The Journal of Immunology 1996, 157 (8), 3270–3279. [PubMed: 8871621]

(56). Riet IV; Waele MD; Remels L; Lacor P; Schots R; Camp BV Expression of Cytoadhesion Molecules (CD56, CD54, CD18 and CD29) by Myeloma Plasma Cells. British Journal of Haematology 1991, 79 (3), 421–427. 10.1111/j.1365-2141.1991.tb08050.x. [PubMed: 1721526]

(57). Bui TM; Wiesolek HL; Sumagin R ICAM-1: A Master Regulator of Cellular Responses in Inflammation, Injury Resolution, and Tumorigenesis. J Leukoc Biol 2020, 108 (3), 787–799. 10.1002/JLB.2MR0220-549R. [PubMed: 32182390]

(58). Derksen PWB; Keehnen RMJ; Evers LM; van Oers MHJ; Spaargaren M; Pals ST Cell Surface Proteoglycan Syndecan-1 Mediates Hepatocyte Growth Factor Binding and Promotes Met Signaling in Multiple Myeloma. Blood 2002, 99 (4), 1405–1410. 10.1182/blood.v99.4.1405. [PubMed: 11830493]

(59). Lozovatsky L; Abayasekara N; Piawah S; Walther Z CASK Deletion in Intestinal Epithelia Causes Mislocalization of LIN7C and the DLG1/Scrib Polarity Complex without Affecting Cell Polarity. Mol Biol Cell 2009, 20 (21), 4489–4499. 10.1091/mbc.e09-04-0280. [PubMed: 19726564]

(60). Gujral TS; Karp ES; Chan M; Chang BH; MacBeath G Family-Wide Investigation of PDZ Domain-Mediated Protein-Protein Interactions Implicates β-Catenin in Maintaining the Integrity of Tight Junctions. Chem Biol 2013, 20 (6), 816–827. 10.1016/j.chembiol.2013.04.021. [PubMed: 23790492]

(61). Shin K; Wang Q; Margolis B PATJ Regulates Directional Migration of Mammalian Epithelial Cells. EMBO Rep 2007, 8 (2), 158–164. 10.1038/sj.embor.7400890. [PubMed: 17235357]

(62). Barreda D; Ramón-Luing LA; Duran-Luis O; Bobadilla K; Chacón-Salinas R; Santos-Mendoza T Scrib and Dlg1 Polarity Proteins Regulate Ag Presentation in Human Dendritic Cells. J Leukoc Biol 2020, 108 (3), 883–893. 10.1002/JLB.4MA0320-544RR. [PubMed: 32293058]

(63). Heider M; Eichner R; Stroh J; Morath V; Kuisl A; Zecha J et al. The IMiD Target CRBN Determines HSP90 Activity toward Transmembrane Proteins Essential in Multiple Myeloma. Mol Cell 2021, 81 (6), 1170–1186.e10. 10.1016/j.molcel.2020.12.046. [PubMed: 33571422]

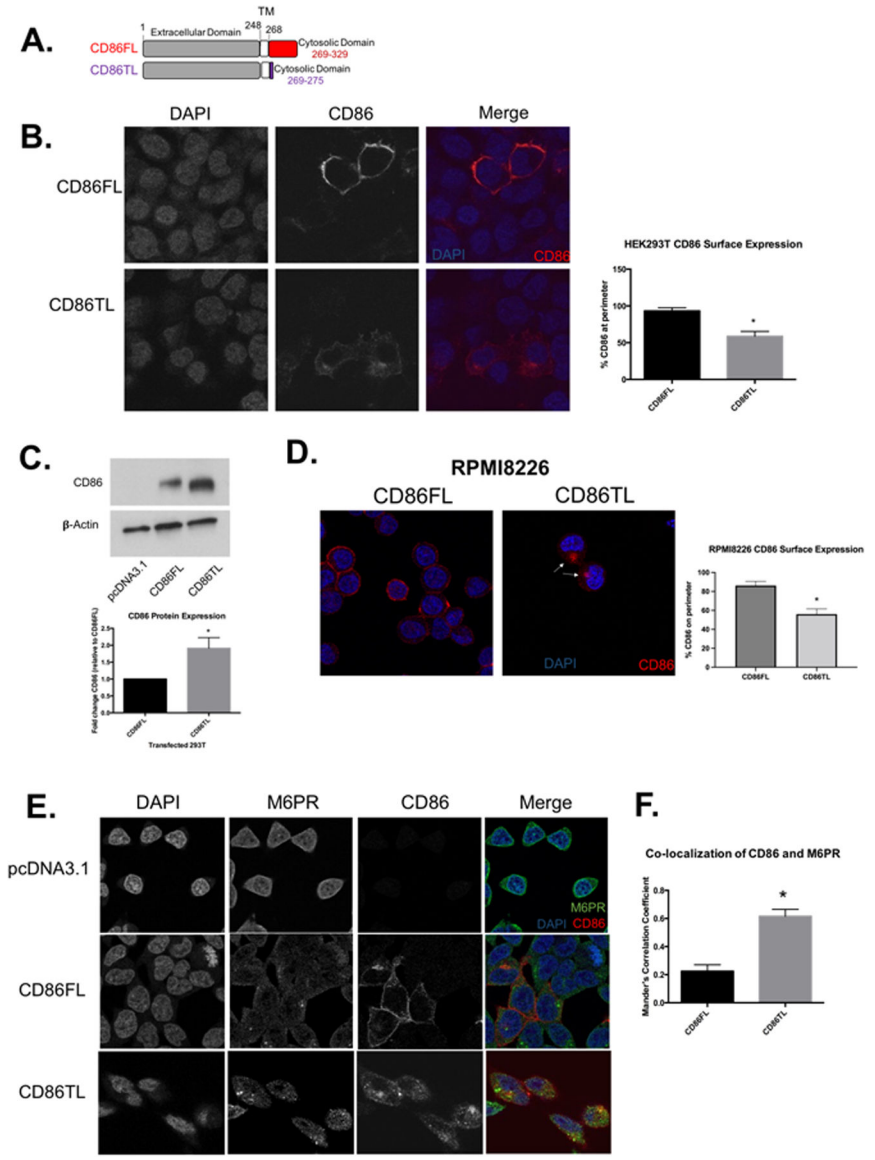

Figure 1: CD86 cytoplasmic tail is important for trafficking to cell surface

(A) Diagram of full length CD86 (CD86FL) and a “tail-less” CD86 (CD86TL) which lacks all but 7 amino acids of the cytosolic domain. TM refers to transmembrane domain. (B) Confocal microscopy analysis of HEK293T cells transfected for 48h with either CD86FL or CD86TL constructs. In merge images, blue staining denotes DAPI nuclear staining, and red staining denotes CD86. Quantification of percentage of CD86 at the perimeter of the cells shown on right. Data quantification are representative of 15 individual cells taken from 3 independent experiments. (C) Protein lysates of HEK293T transfected with either empty vector pcDNA3.1, CD86FL or CD86TL were subjected to sodium dodecyl sulfate–polyacrylamide gel electrophoresis (SDS-PAGE) followed by western blotting using anti-CD86 and anti β-actin antibodies. Quantification of CD86 expression in CD86FL and CD86TL transfected HEK293T. CD86 protein expression was normalized to β-actin expression and then normalized to CD86FL protein expression.

N=3. (D) Confocal microscopy of RPMI8226 lines stably overexpressing either full-length (CD86FL) or tail-less CD86 (CD86TL). Blue staining denotes DAPI nuclear staining while red staining denotes CD86. Arrows refer to regions of punctate CD86 expression in CD86TL. Quantification of percentage of CD86 at the perimeter of the cells shown on right. Data representative of 3 independent experiments. (E) HEK293T cells transfected for 48h with either pcDNA3.1, CD86FL or CD86TL constructs and co-stained with CD86 and Mannose-6 Phosphate Receptor (M6PR). In merge images, blue staining denotes DAPI nuclear staining, green staining denotes M6PR, and red staining denotes CD86. (F) Mander's Correlation Coefficient was used to determine co-localization of M6PR with CD86 in CD86FL and CD86TL HEK293T cells. This reports findings from 15 individual cells taken from 3 independent experiments *$p<0.05$

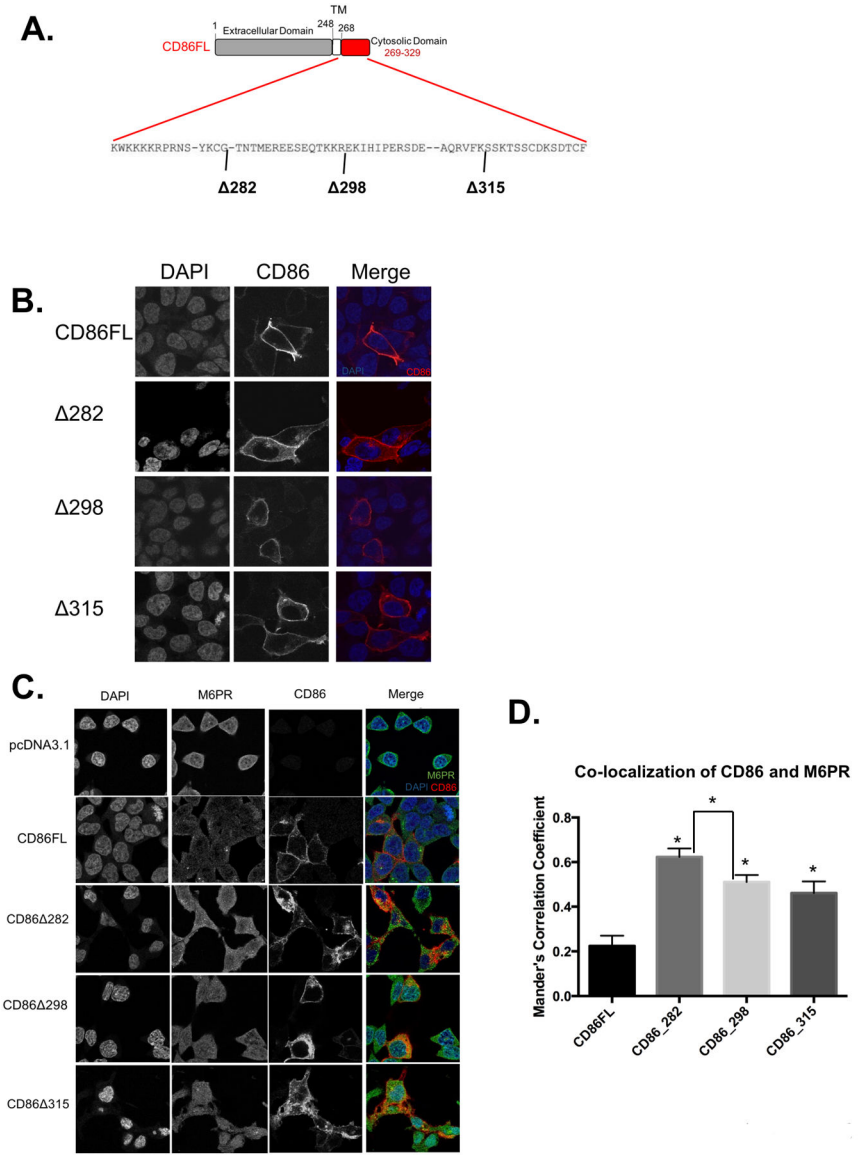

Figure 2: Multiple Regions of CD86 cytoplasmic tail are important for trafficking to cell surface

(A) Diagram of CD86 cytoplasmic region and truncation mutants. Δ282 refers to truncated CD86 containing 282 amino acids. Δ298 and Δ315 refer to truncated CD86 containing 298 and 315 amino acids respectively. (B) Confocal microscopy analysis of HEK293T cells transfected for 48h with either CD86FL, Δ282, Δ298, or Δ315 constructs. In merge images, blue staining denotes DAPI nuclear staining, and red staining denotes CD86. Data are representative of 3 independent experiments. (C) HEK293T cells transfected for 48h with either empty vector pcDNA3.1, CD86FL or CD86 truncation mutant constructs were co-stained with CD86 and M6PR. In merge images, blue staining denotes DAPI nuclear staining, green staining denotes M6PR, and red staining denotes CD86. (D) Mander's Correlation Coefficient was used to determine co-localization of M6PR with CD86 in CD86FL, CD86Δ282, CD86Δ298, and CD86Δ315 HEK293T cells. The graph represents results from 15 individual cells analyzed from 3 independent experiments. *p<0.05

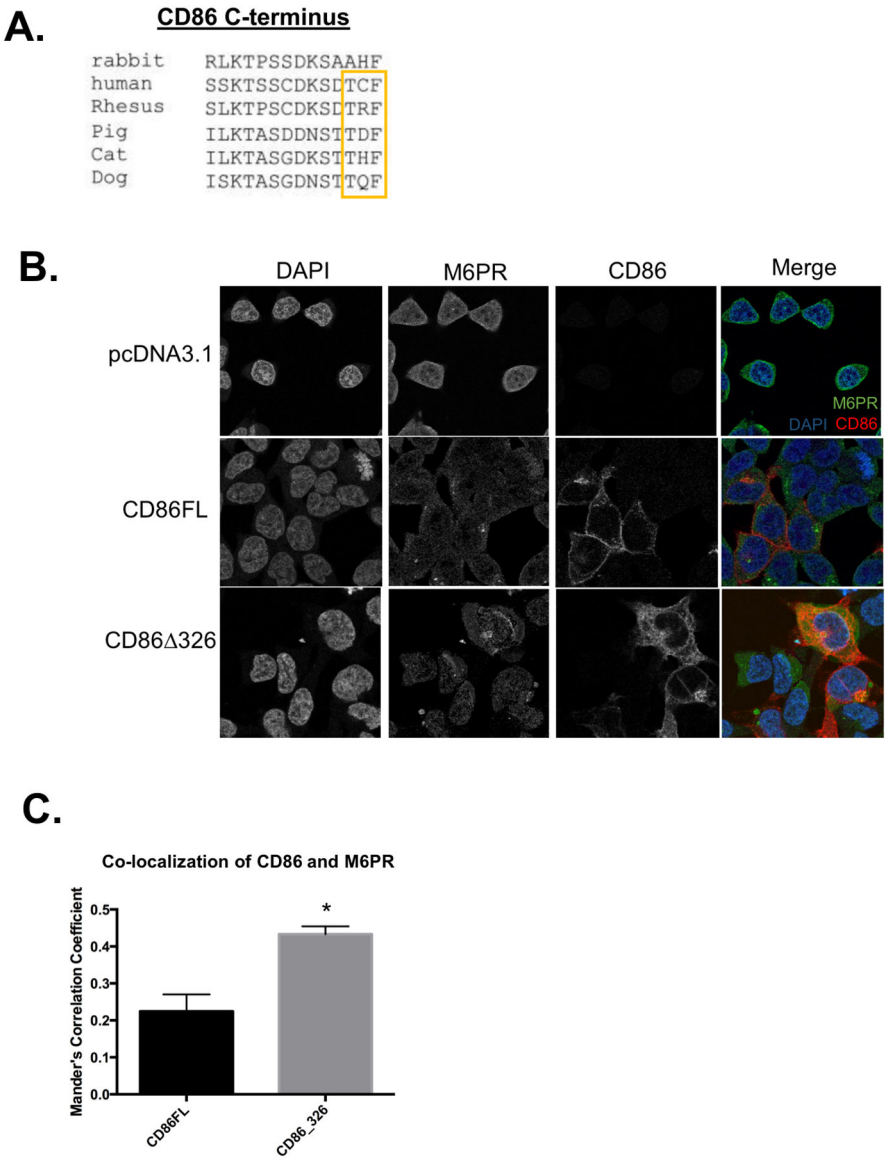

Figure 3: CD86 contains a PDZ binding motif important for surface expression

(A) Alignment of the 14 amino acids at the C-terminus of CD86. Highlighted is the conserved Class I PDZ binding domain. (B) HEK293T cells transfected for 48h with either empty vector pcDNA3.1, CD86FL or CD86 truncation mutant constructs lacking the PDZ binding motif (CD86Δ326) were co-stained with CD86 and Mannose-6 Phosphate Receptor (M6PR). In merge images, blue staining denotes DAPI nuclear staining, green staining denotes M6PR, and red staining denotes CD86. (C) Mander's Correlation Coefficient was used to determine co-localization of M6PR with CD86 in CD86FL and CD86Δ326 HEK293T cells. The graph represents results from 15 individual cells analyzed from 3 independent experiments. *p<0.05

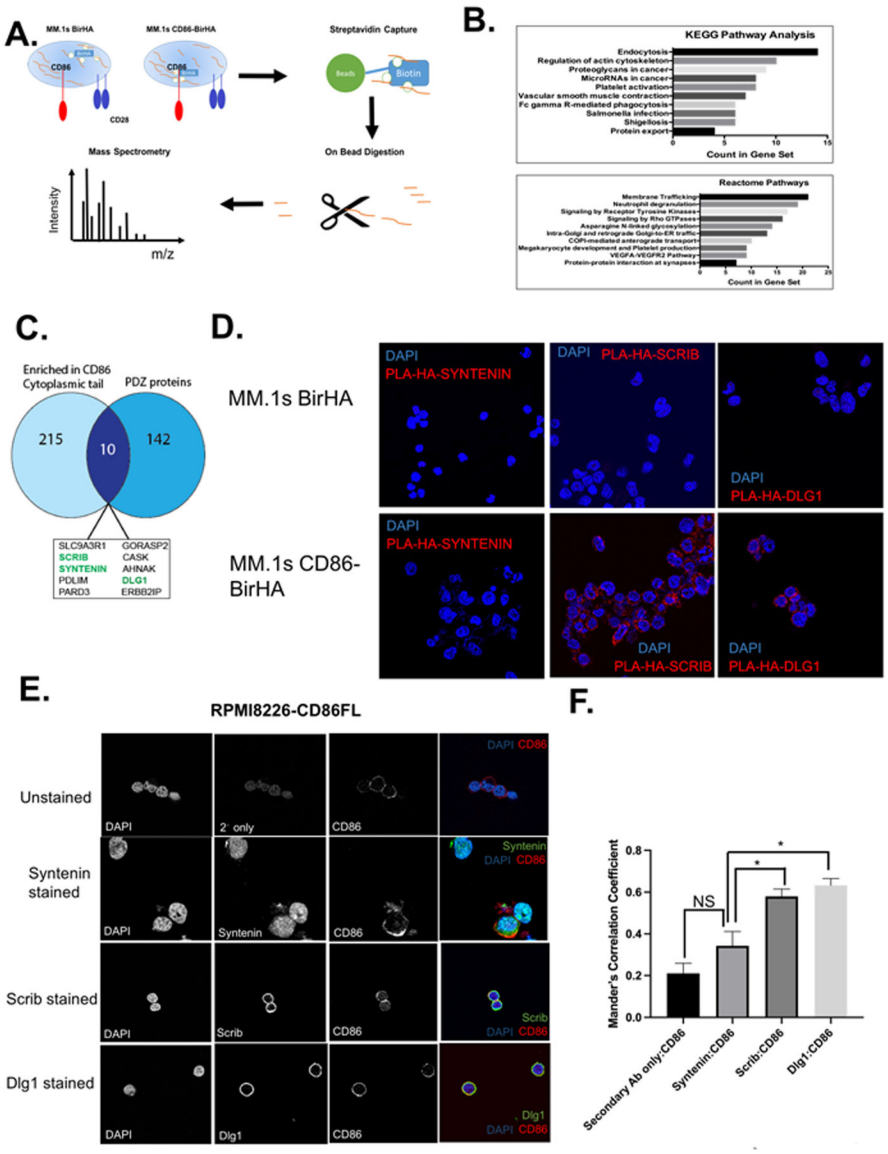

Figure 4: BioID proximity assay identifies numerous CD86 cytoplasmic tail interacting partners

(A) Schematic of study design: MM.1s cells stably expressing soluble BirHA control or CD86-BirHA were cultured with 50μM biotin, lysed, and quantified. Biotinylated proteins were then captured using equal amounts of streptavidin beads. Peptides were generated via on bead digestion, and these resulting peptides were then purified and analyzed by LC-MS. (B) Gene ontology KEGG pathway analysis and Reactome Pathway analysis of the high confidence CD86 cyotplasmic tail binding partners. (C) Venn Diagram of CD86 cytoplasmic tail enriched proteins and PDZ-domain proteins determined from the HUGO nomenclature database. (D) Interaction between SYNTENIN, SCRIB, or DLG1 with CD86 (MM.1s CD86-BirHA) or soluble BirHA control (MM.1s BirHA) were analyzed by PLA. Blue staining denotes DAPI nuclear staining, red staining denotes PLA staining. (E) RPMI8226 cells stably overexpressing CD86FL (RPMI8226-CD86FL) were co-stained with CD86 and either SYNTENIN, SCRIB, DLG1 or a secondary antibody only control. In merge

images, blue staining denotes DAPI nuclear staining, green staining denotes SYNTENIN/SCRIB/DLG1, and red staining denotes CD86. Data are representative of 3 independent experiments. (F) Mander's Correlation Coefficient was used to determine co-localization of SYNTENIN/SCRIB/DLG1 with CD86 in RPMI8226-CD86FL as well as cells stained only with a secondary antibody. The graph represents results from 15 individual cells analyzed from 3 independent experiments. *$p<0.05$

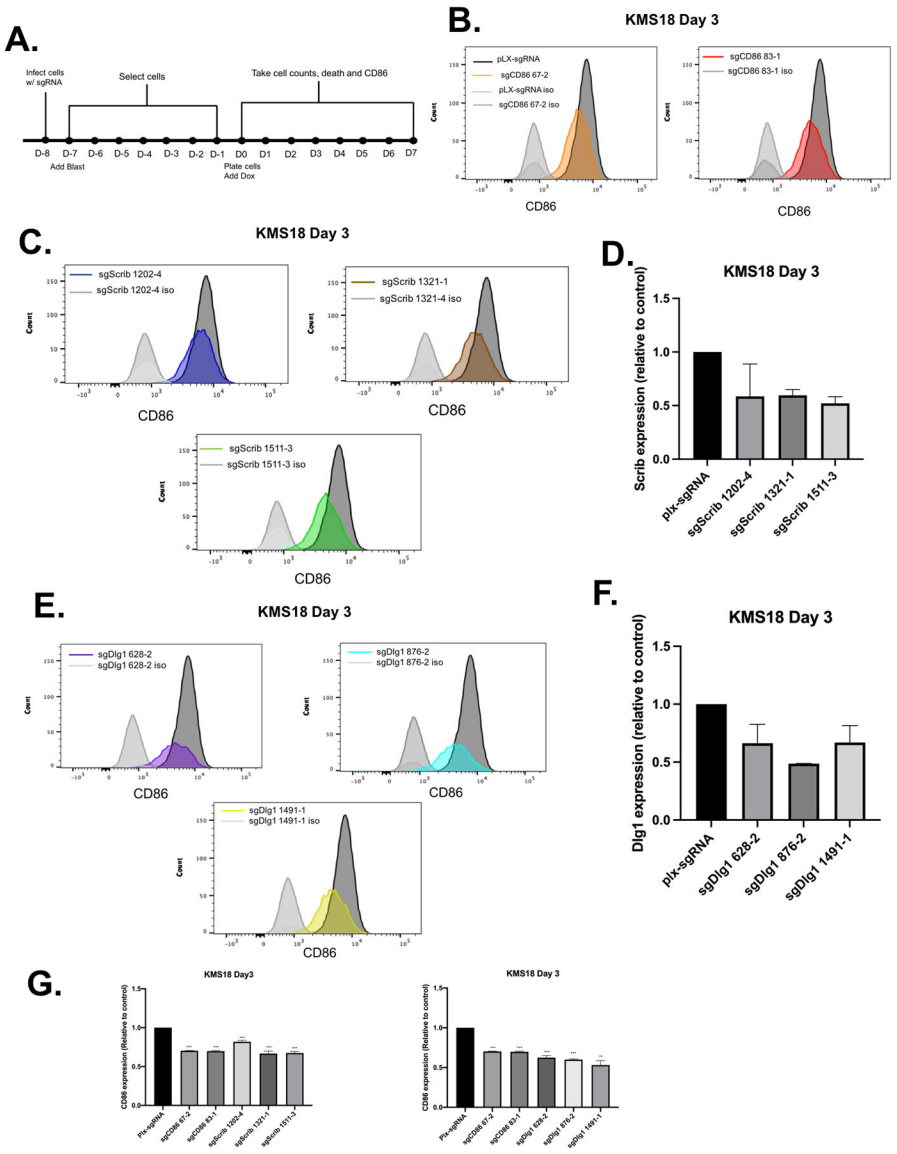

Figure 5: SCRIB and DLG1 regulate CD86 surface expression

(A) Study design: Doxycycline-inducible Cas9 containing KMS18 or RPMI8226 myeloma cells were infected with lentiviral particles containing CRISPR single guide RNA (sgRNA) targeting coding regions in SCRIB (1202–4, 1321–1, 1511–3), DLG1 (628–2, 876–2, 1491–1) or a control sgRNA targeting the viral incorporation site AAVS1 (plx-sgRNA). The next day, blasticidin was added to select cells for seven days. Following this, doxycycline was added to activate the Cas9 enzyme and cell counts, cell death, and CD86 expression were measured from days 0–7. (B,C,E) Representative histograms showing CD86 surface expression was measured via flow cytometry three days after doxycycline addition for (*B)* sgCD86, (*C*) *sgSCRIB*, and (*E)* sgDLG1 KMS18 cells. (D,F) mRNA expression for plx-sgRNA and (*D*) SCRIB and (*F)* DLG1 sgRNA guides were measured using quantitative reverse transcription PCR (qRT-PCR) 3 days after doxycycline addition in KMS18 cell lines. (G) Quantification of CD86 surface expression for 3 independent experiments 3 days after

doxycycline addition in plx-sgRNA, sgCD86, sgSCRIB (left) and sgDLG1 (right) in KMS18 myeloma cell line. N=3, *p<0.05, **p<0.01

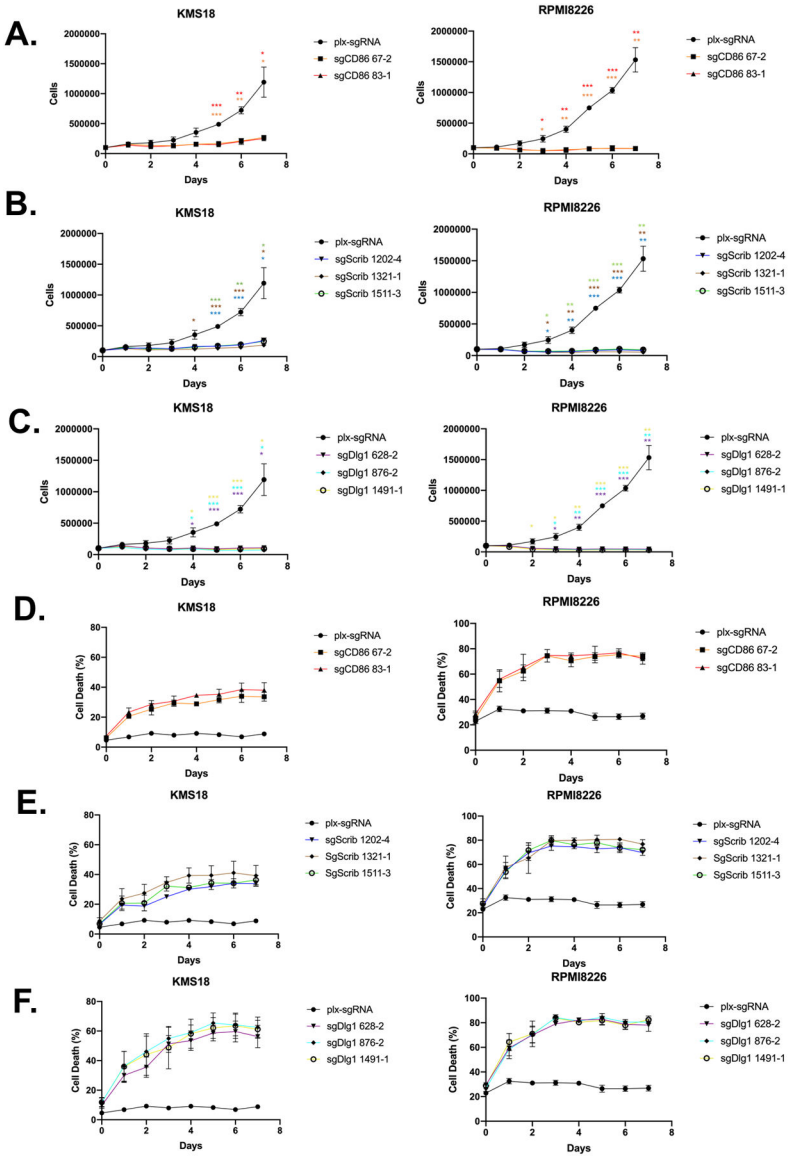

Figure 6: SCRIB and DLG1 are important for cell growth and viability

(A-C) Doxycycline inducible Cas9 containing KMS18 or RPMI8226 myeloma cell lines were infected with lentiviral particles containing CRISPR single guide RNA (sgRNA) targeting exons in CD86 (67–2, 83–1) SCRIB (1202–4, 1321–1, 1511–3), DLG1 (628–2, 876–2, 1491–1) or a control sgRNA targeting the viral incorporation site AAVS1 (plx-sgRNA). After blasticidin selection for seven days, doxycycline was added and cell counts were assessed for Day 0–7. (A) Counts of plx-sgRNA control cells with sgCD86. (B) Counts of plx-sgRNA control cells with sgSCRIB. (C) Counts of plx-sgRNA control cells with sgDLG1 cells. (D-F) Annexin V–fluorescein isothiocyanate and propidium iodide staining staining was used to assess cell viability in KMS18 and RPMI8226 cell lines receiving either plx-sgRNA, sgCD86, sgSCRIB, or sgDLG1 guides for day 0–7 following doxycycline treatment. (D) Cell death of plx-sgRNA control cells with sgCD86 cells. (E) Cell death of

plx-sgRNA control cells with sgSCRIB cells. (F) Cell death of plx-sgRNA with sgDLG1 cells. N=3, *p<0.05, **p<0.01, ***p<0.001

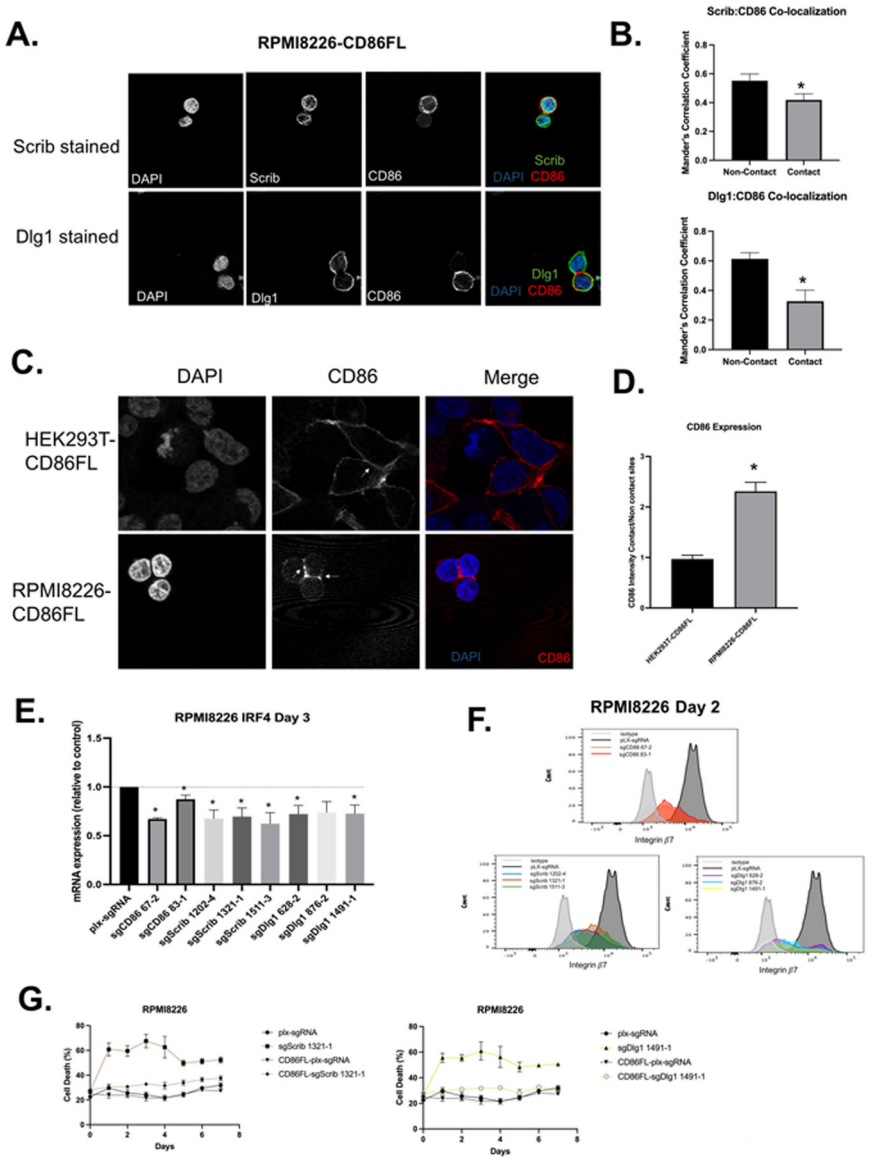

Figure 7: SCRIB and DLG1 regulate CD86 prosurvival signaling

(A) RPMI8226-CD86FL cells were co-stained with CD86 and either SCRIB (top) or DLG1 (bottom). In merge images, blue staining denotes DAPI nuclear staining, green staining denotes SCRIB/DLG1, and red staining denotes CD86. (B) Mander's Correlation Coefficient was used to determine co-localization of SCRIB/DLG1 with CD86 in areas of cell-cell contact compared to areas of no contact between adjacent RPMI8226 cells. The graph represents results from 15 individual cells analyzed from 3 independent experiments. (C) Confocal microscopy analysis of HEK293T cells transfected for 48h with CD86FL and RPMI8226 cells stably overexpressing CD86FL. In merge images, blue staining denotes DAPI nuclear staining and red staining denotes CD86. (D) Ratio of relative intensity of CD86 staining was determined between areas of cell contact and non-contact between adjacent CD86FL-transfected HEK293T and RPMI8226-CD86FL cells. The graph represents results from 15 individual cells analyzed from 3 independent experiments. (E)

mRNA expression of IRF4 for plx-sgRNA, CD86, SCRIB, and DLG1 sgRNA guides were measured using quantitative reverse transcription PCR (qRT-PCR) 3 days after doxycycline addition in RPMI8226 cell lines. N=3. (F) Surface Integrin β7 levels were measured in RPMI8226 for sgCD86 (left), sgSCRIB (center), and sgDLG1 (right) 2 days after doxycycline addition. Data are representative of 3 independent experiments. (G) Cell viability in RPMI8226 or CD86FL-overexpressing RPMI8226 cell lines receiving either plx-sgRNA, sgSCRIB, or sgDLG1 guides for day 0–7 following doxycycline treatment. N=3, *$p<0.05$